SolarPACES 2024, 30th International Conference on Concentrating Solar Power, Thermal, and Chemical Energy Systems

Analysis and Simulation of CSP and Hybridized Systems

https://doi.org/10.52825/solarpaces.v3i.2344

Published: 26 Jan. 2026

System-Level Assessment of Green Hydrogen Production via SOEC-Solar Thermal Integration

Ignacio Javier Arias[1], Felipe G. Battisti[2], Armando Castillejo Cuberos[1], José Alfonso Romero-Ramos[3], Loreto Valenzuela[4], Luis Francisco González-Portillo[5], José Cardemil[1], and Rodrigo Escobar[1]

[1]Departamento de Ingeniería Mecánica y Metalúrgica, Escuela de Ingeniería Pontificia Universidad Católica de Chile, Chile

[2]Departamento de Ingeniería Mecánica, Facultad de Ingeniería, Universidad Tecnológica Metropolitana, Chile

[3]Centro de Investigación en Energía Solar (CIESOL), Centro Mixto UAL-CIEMAT, Universidad de Almería, España

[4]CIEMAT, Plataforma Solar de Almería, España

[5]Departamento de Ingeniería Energética, Universidad Politénica de Madrid, España

*Correspondence: Ignacio Arias, ivarias@uc.cl

Abstract. This study investigates the integration of third-generation (Gen3) Concentrated Solar Power (CSP) systems with Solid Oxide Electrolysis Cells (SOEC) for green hydrogen (gH2) production in the Atacama Desert, Chile. A 100 MW CSP plant coupled with SOEC systems of varying capacities is modeled to optimize hydrogen production using thermal storage particles at 780°C. The analysis focuses on the techno-economic performance, highlighting the importance of Thermal Energy Storage (TES) capacity. Results indicate that optimal gH2 production occurs with around 10 hours of TES, be- yond which additional storage offers minimal benefits. The findings demonstrate that asymmetrical capacity integration between CSP and SOEC systems is economically advantageous, particularly when maintaining a capacity ratio (CR) between 0.01 and 0.2. This integration can potentially exceed the energy demands of the region's copper mining industry, contributing to significant reductions in fossil fuel reliance and promoting the commercialization of surplus hydrogen.

Keywords: Green Hydrogen, Concentrated Solar Power, Electrolyzers, Solar Energy

1. Introduction

The transition to a decarbonized energy matrix is critical to limiting global temperature rise to 1.5°C. Despite global efforts, fossil fuels accounted for 78.5% of global energy consumption in 2021, with only 12.6% from renewable sources [1]. This gap is particularly significant in sectors like heavy transportation and chemical industries, where high-energy-density vectors such as gH_2 are essential. In response, Chile has focused on increasing the penetration of gH_2 into its national energy matrix, necessitating research, development, and regulatory frameworks to support its production and integration across various productive sectors. Currently, efforts are concentrated on decarbonizing the copper mining industry, which accounts for 35% of the country's electricity demand and around 15% of total energy demand when including fossil fuels. Therefore, evaluating cost-effective methods for producing gH_2 from renewable energy is crucial for assessing technological options and estimating national gH_2 requirements.

Water splitting methods using renewable energy provide a CO2-free pathway for hydrogen production. SOECs are particularly promising for efficient hydrogen production and integration with high temperature processes, especially in synergy with CSP technologies. However, the $LCOH_2$ achieved with SOEC systems coupled with thermal sources (nuclear, solar, wind, or high-temperature waste heat) still exceeds the International Energy Agency's 2030 target, requiring further technological advancements for cost reduction. Integrating SOEC with Gen3 CSP plants using solid particles for steam production enhances overall efficiency, as these particles can be heated near the optimal SOEC operating temperature (800°C). Nonetheless, challenges such as heat loss and component durability under extreme conditions persist. This study conducts a techno-economic and performance analysis of a CSP+SOEC system for hydrogen production in two specific conditions: the extremely arid Atacama Desert and the high-density mining areas in Chile. Through dynamic modeling, this research addresses existing gaps and provides insights into hydrogen production and its potential to replace fossil fuels in the evaluated region, advancing the understanding of CSP+SOEC integration.

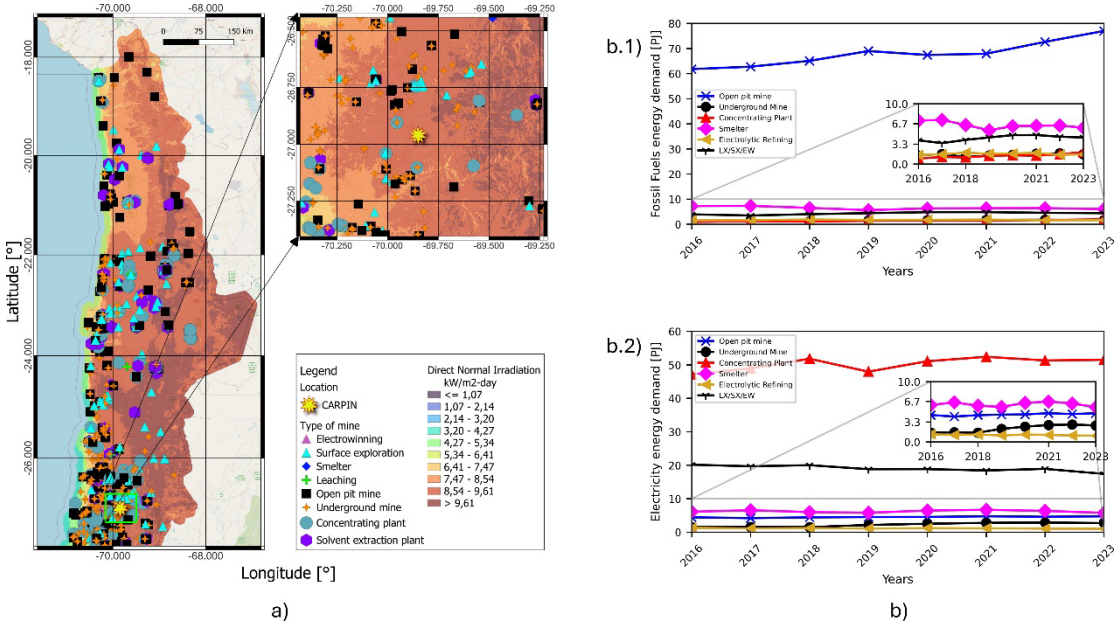

Figure 1. *(a) Contrast of the location under study concerning to the daily direct normal irradiation potential, and the copper mining activity density in northern Chile and (b) illustration of annual energy demand by source of copper mining industry in Chile*

2. Methodology

2.1 Location under study

This study evaluates gH_2 production via SOEC-Solar Thermal integration in northern Chile, focusing on Carrera Pinto (CARPTO) in the Atacama region. Meteorological data from Solcast (2013-2022) was used to create TMY-P50 datasets with hourly resolutions. Carrera Pinto, situated at 1,915 meters above sea level, was chosen for its high solar radiation and proximity to industrial hubs, particularly large-scale copper mining. This region, representing about 10.2% of Chile's electricity demand and around 10.7 % of total energy demand, is crucial for decarbonizing the mining sector. Fig. 1 highlights the site's strategic location relative to mining activities and solar potential.

2.2 System descriptions and modeling considerations

The OpenModelica (OPM) software was used as the simulation platform, incorporating various Modelica Standard Library packages, including Fluid, Math, and Media, along with external

libraries like SolarTherm and Chemical. The modeled system is a solid-particle Gen3 CSP with a recompression supercritical carbon dioxide (sCO_2) Brayton cycle as the power block (PB). It has a nominal capacity of 100 MWe and a solar multiple (SM) of 3, with TES capacity sensitized between 4 and 20 hours. The design point is set for the summer solstice at solar noon with a direct normal irradiance (DNI) of 950 W/m^2, a concentration factor of 2000, and PB efficiency of 51% [2]. Regarding this last parameter, it is worth noting that there is no consensus in the literature regarding the optimal design point. Since the cycle thermal efficiency depends on the compressor inlet temperature, which in turn is influenced by ambient temperature, the overall efficiency varies dynamically throughout the simulation time steps. Authors such as González-Portillo et al. [3] and Gan et al. [4] have proposed design thermal efficiencies around 50% to 50.5% for operating ranges similar to those considered in this work, whereas J. Chen et al. [5] has reported operational thermal efficiencies of approximately 52% even for turbine inlet temperatures around 700°C. These findings suggest that adopting a design thermal efficiency between 50% and 51% is a conservative and appropriate assumption for this type of analysis. Meanwhile, the nominal capacity of the integrated SOEC system was defined as a fraction of the CSP capacity through CR, allowing evaluation on different scales.

The solid-particle Gen3 CSP system model uses CARBO HSP 40/70 as the heat transfer medium, with a one-aperture free-falling (1AFF) particle receiver, ground-based TES bins, lifts, and a supercritical CO_2 Brayton cycle as the PB. Custom models, including a 1-D 1AFF particle receiver, storage containers, and a particle lift mechanism, were integrated into OPM to simulate the energy behavior of the system. Solar geometry and heliostat field modeling were handled using SolarTherm's ”Sun” and ”HeliostatsField” models, applying the PSA solar position algorithm to determine solar angles and using a steady-state model for concentrated radiation flux [6]. The optical efficiency of the solar field was calculated using a bivariate Akima interpolation of a two-dimensional optical efficiency lookup table. The 1-D 1AFF modeling considers the discretization of the aperture area into ten nodes and includes heat transfer phenomena such as advection, radiation and convection [7]. Meanwhile, the power block's behavior was simulated using correlations from the sCO2CycleNREL class in SolarTherm, which considers ambient temperature, mass flow rate variation, and inlet temperature to compute the heat flow, gross energy production, and net power output.

The SOEC system is comprised of several critical components: a main feed water pumping system (Pump1), a secondary pump specifically for the electrolyzer (Pump2), and a tertiary pump that handles the cooling of the compressor (Pump3). Additionally, the system includes a recovery water pump (Pump4), a gas/water separator, and two tanks—designated as control volumes CV1 and CV2 — responsible for main and recovery water storage, respectively. The SOEC stacks are integrated with a multistage compression system (MSC) and a three-level override control system. Heat management is achieved through a network of heat exchangers, including an evaporator (HX1), a heater (HX2) for heat recovery, and a superheater (HX3). Particularly, the SOEC stack model is based on the electrochemical dynamic model reported by Ni et el. [8]. Which has been improved considering the diffusion kinetics of the chemical species according to the guideline proposed by Zhang et al. [9].

On the other hand, the heat exchanger system was designed with a pinch point of 20 °C between the steam outlet and particle inlet temperatures (800 °C), aiming for a solid-particle outlet temperature of 540 °C at HX3, suitable for returning to the low- temperature bin. HX1 was designed with a 15 °C pinch point between water inlet and outlet temperatures, with the water entering the electrolysis process at 20 °C. HX2 features a 40 °C pinch point between the steam inlet and hydrogen outlet temperatures. Despite the separation of chemical species during electrolysis, the inlet temperatures for steam and hydrogen in HX1 and HX2 are set at 780°C, determined by the exit temperature of HX3. The compression system operates at a dispatch pressure of 80 bar, ideal for industrial transportation and processing.

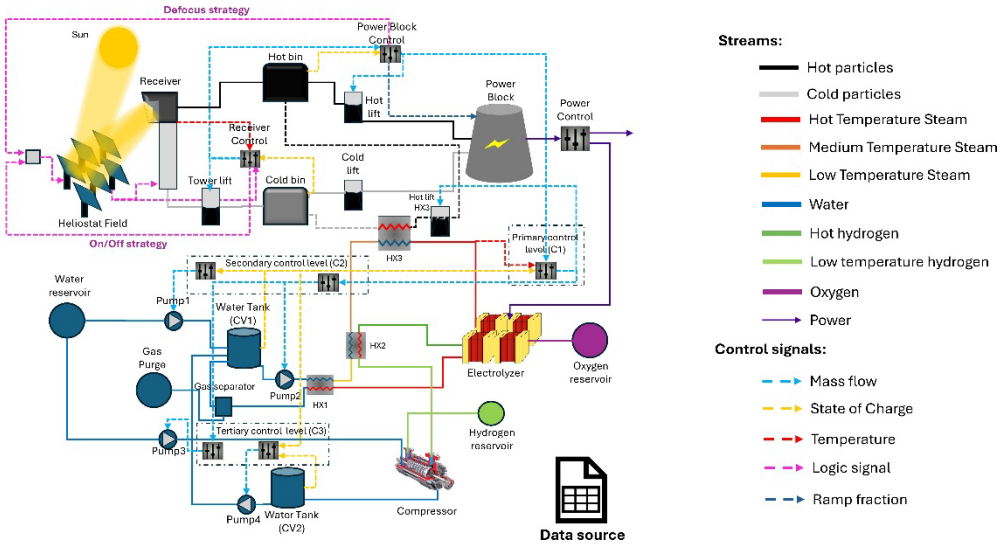

Figure 2. *System-Level approach developed in OpenModelica*

The CSP plant's control system optimizes the mass flow of solid particles between the PB and the receiver, adapting to fluctuations in solar radiation through a three-stage proportional-integral (PI) control system. This regulation maintains specific temperature targets at the receiver's outlet, ensuring efficient operation and enhanced energy production under varying solar conditions. The PB control system operates in four modes—off, standby, partial load, and full load—allowing flexible energy management based on demand. Additionally, solar field control is linked to particle levels in the hot and cold bins, with operations modulated by thresholds for sunlight intensity (DNI) and wind speed, ensuring operation only under favorable conditions. The SOEC system is integrated with the CSP system via a three-level override control. The primary level manages solid-particle flow through the heat exchanger and electricity supply to the SOEC, ensuring operation only under optimal conditions. The secondary level regulates water flow and storage, adjusting pump operations based on storage tank levels. The tertiary level monitors charge levels in two storage tanks, coordinating water recovery and pump operations to maintain system balance. This comprehensive control strategy ensures continuous and efficient CSP plant operation despite solar energy variability. Fig. 2 illustrates the system-level approach developed within OPM.

2.3 Techno-economic assumptions

The techno-economic analysis evaluated three key indicators: LCOE, LCOH, and $LCOH_2$. LCOE and $LCOH_2$ were calculated following the methodology by Arias et al. [10], while LCOH was computed similarly to LCOE, focusing on the annual heat absorbed and stored in the hot bin and related subsystems for these purposes. The analysis adhered to guidelines from the US Department of Energy (DOE) via SANDIA National Laboratories [11], considering parameters like a 4.4% real discount rate, 2.5% annual inflation, a 30-year plant lifespan, and a 0-year construction period. These parameters ensure consistency, abstracting from variations in the literature and accounting for real-world dynamics. The cost structure and functions from Refs. [3], [4] were used to estimate LCOE and LCOH for the solid-particle Gen3 CSP plant. Meanwhile, for SOEC system the cost structure followed by Arias et al. [2] was used. Operational expenses (OPEX), both fixed and variable, were tailored to the specific scenarios and technolog- ical differences between CSP and SOEC systems. The SOEC system's annual costs for electricity and water were based on a power purchase agreement (PPA) at LCOE and a water cost of 3.1 USD/m^3, reflecting local conditions in Chile [10]. The analysis used a bottom-up specific cost of 300 USD/kW_{dc} for the SOEC stack [12], with sensitivity to lower costs of 100 and 50 USD/kW_{dc}, as targeted by Prosser et al. [13] and the DOE [14], aiming for an LCOH2 as low as 1 USD/kg-H2 by 2031. Thus, Table 1, and Table 2 summarized the cost structure used for the Gen3 CSP and SOEC systems, respectively.

Table 1. *Economic assumptions and specific costs for Gen3 CSP system*

Parameter	Value	Unit	Refs.
Real discount rate	4.4	%	[3], [4]
Inflation rate	2.5	%	[3], [4]
Lifetime of the plant	30	years	Assumed
Time of construction	0	years	Assumed
State subsidies	0	$	Assumed
Contingency (of CAPEX)	10	%	[3], [4]
EPC (of CAPEX)	9	%	[3], [4]
Fixed O&M cost	40	USD/W	[3], [4]
Variable O&M cost	3	USD/MWh	[3], [4]
Balance of Plant cost	0.167	USD/kWe	[3], [4]
Field cost	75	USD/m^2	[3], [4]
Site preparation cost	10	USD/m^2	[3], [4]
Land cost	2.471	USD/m^2	[3], [4]
Receiver	37400	USD/m^2	[3], [4]
Tower	see table notes	USD/m	-
Lifts	58.37	USD/m*(kg/s)	[3], [4]
Refractory material	2700	USD/m3	[4]
High density concrete	850	USD/m3	[4]
Portland concrete	229	USD/m3	[4]
Floor filler material	150	USD/m3	[4]
Solid-Particle CARBO HSP 40/70	1	USD/kg	[4]
Power block	see the cost function in the reference	USD/kWe	[2]

Table 2. *Economic assumptions and specific costs for SOEC system*

Parameter	Value	Unit	Refs.
SOEC stack system	300, 100, and 50	USD/kWe	[12]
Compressors	40035	USD/kWe^0.6038	[15]
Pumps	705.48	USD/kWe^0.71	[15]
Gas separator vessel	40	USD/kWe	[16]
Water tank	200	USD/m^3	-
Electronic and control systems	40	USD/kWe	[12]
Primary heat exchanger (HX3)	1000	USD/m^2	[3], [4]
Heat exchangers HX1 and HX2	32.8	USD/m^2	[15]
BoP cost	175	USD/kWe	[12]
Water	3.1	USD/m^3	-
Electricity	valued at LCOE	USD/MWh	-
Heat	valued at LCOH	USD/MWh	-
Fixed O&M CAPEX rate cost	2	%	-
Site preparation cost	10	USD/m^2	[3], [4]
Stack lifetime	90000	h	[12], [14]
Stacks replacement rate	30	%	[12], [14]

3. Results and discussion

Based on the climatological data, modeling aspects, and techno-economic assumptions, the daily and annual performance of the system was characterized. Fig. 3 shows the behavior of a 25 MW_{dc} SOEC system coupled to a 100 MW CSP plant with 8 h of TES capacity and a SM of 3, over two days in summer and winter at CARPTO using a five-minute TMY-P50 dataset. The CSP system's behavior is depicted by the heat absorbed by the receiver ($\dot{Q}_{rcv}$), the state of charge (SoC) of the hot-bin storage, and the nominal output power of the PB (W_{net}). The SOEC system's key parameters are represented by the electrical efficiency of the electrolyzer (η_{soec}) (black line). The figure highlights the SOEC system's full dependence on the CSP system, driven by its electrical power needs from the PB and the heat flux from the TES system. This results in a coordinated and parallel operation, where both systems are integrated yet controlled independently from the CSP system's control scheme.

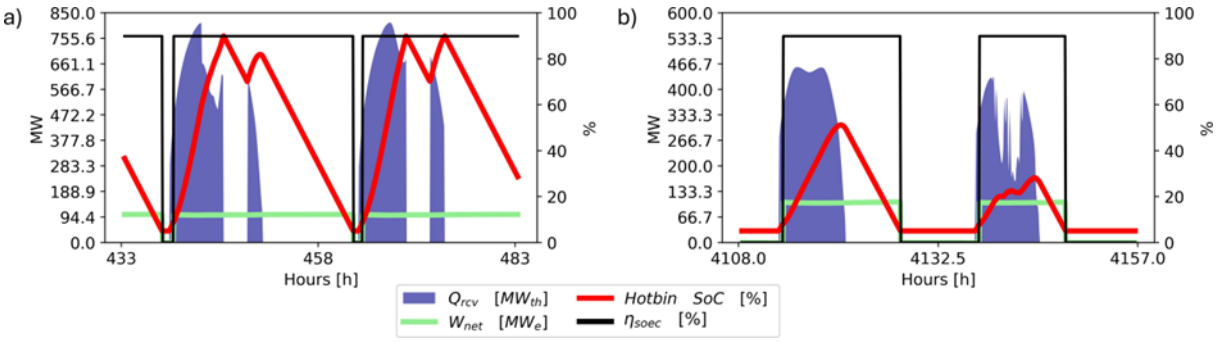

Figure 3. *Illustration of the behavior of a 25 MW_{dc} SOEC system coupled to a Gen3 CSP plant of 100 MWe with SM=3 and 8h of TES for 2 days of (a) summer and (b) winter*

The TES system plays a crucial role in steam generation for electrolysis, extending CSP operation during low DNI periods and supporting gH_2 production. By maintaining a constant particle flow from the high-temperature container to HX3, a stable heat flow is ensured, optimizing gH_2 output. Fig. 4 shows the daily percentage utilization of TES by the SOEC system compared to daily gH_2 production for a 100 MWe Gen3 CSP plant with 4, 10, and 20 hours of TES capacity and CR values of 0.25, 0.5, and 1. The data indicate that TES utilization by the SOEC system remains below 10% for over 90% of the year, stabilizing around 2% for a CR of 0.25, regardless of TES duration. Increasing TES from 4 h to 10 h improves system dynamics and gH_2 production, particularly in summer, reaching over 20% daily. However, further expansion to 20 h yields marginal gains, less than 5%, benefiting primarily winter operations. This has techno-economic implications, as the cost of higher TES capacities must be weighed against the modest gains in gH_2 output.Fig. 5a illustrates the evolution of annual gH_2 production with TES capacity for various CR values (0.01 to 1). It shows that gH_2 production peaks between 8 h and 12 h of TES, beyond which additional TES capacity offers diminishing returns. This is because larger TES capacity does not necessarily translate to more stored thermal energy, which is needed for steam generation in HX3 and electricity production in the PB. Beyond this point, TES capacity becomes mismatched with the SM, leading to an oversized TES relative to the heat captured by the receiver. Consequently, increasing the solar field beyond an SM of 3 does not justify a larger TES capacity, as it fails to provide additional energy output to offset the higher CAPEX, ultimately reducing the LCOE.

Fig. 5b shows that the minimum LCOE and LCOH values are around 10 h, at approximately 61 USD/MWh and 12.4 USD/MWhth, respectively. Beyond this point, the increased TES capacity does not justify the associated costs.

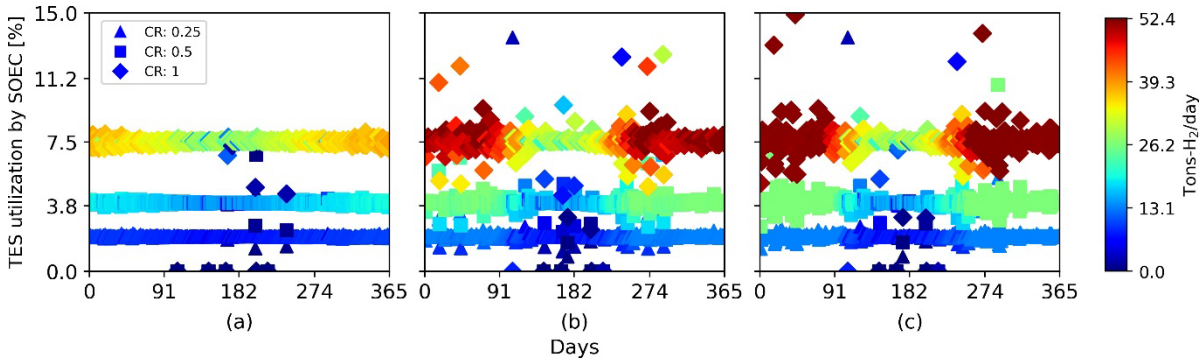

Figure 4. *Exemplification of the daily operation throughout the year represented by the percentage daily TES utilization by SOEC for steam generation in HX3 contrasted with the daily gH2 production for (a) 4h, (b) 10h, and (c) 20h of TES*

Understanding the potential for reducing $LCOH_2$ hinges on key cost scenarios that influence decision-making. According to R. Anghilante et al. [12], the current cost per stack for large-scale systems is around 300 USD/kW_{dc}. While exact timelines are uncertain, with ongoing advancements and increased installations to meet gH_2 demand, costs could decrease to 100 USD/kWdc. The U.S. DOE aims to lower this further to 50 USD/kW_{dc} by 2031. Considering the abovementioned aspects, Fig. 6 illustrates the $LCOH_2$ variation concerning CR and the TES capacity at CARPTO for (a) 300 USD/kW_{dc}, (b) 100 USD/kW_{dc}, and (c) 50 USD/kW_{dc}. This figure illustrates that the contraction in the costs per stack to 100 USD/kWdc and 50 USD/kWdc (a decrease of 66.7% and 83.37% respectively) allows for a decrease in the minimum $LCOH_2$ values to about 3.88 USD/kgH_2 and 3.72 USD/kgH_2. This results in contractions of about 8.3% and 12.1%, respectively. Here it is evident that $LCOH_2$ presents its minimum around 10 h of TES, which is due to the fact that this indicator inherits the trends of LCOE and LCOH due to the concatenation of costs. Additionally, it is observed that this technological integration favors asymmetric integrations in terms of capacities, reflected in CR. Placing the minimum $LCOH_2$ around 0.01<CR<0.2. This is because a SOEC system capacity representing a capacity of up to 20% of the CSP system capacity is less susceptible to power fluctuations, maintaining a daily production practically at nominal load independently of the TES system capacity, as observed in Figure 4.

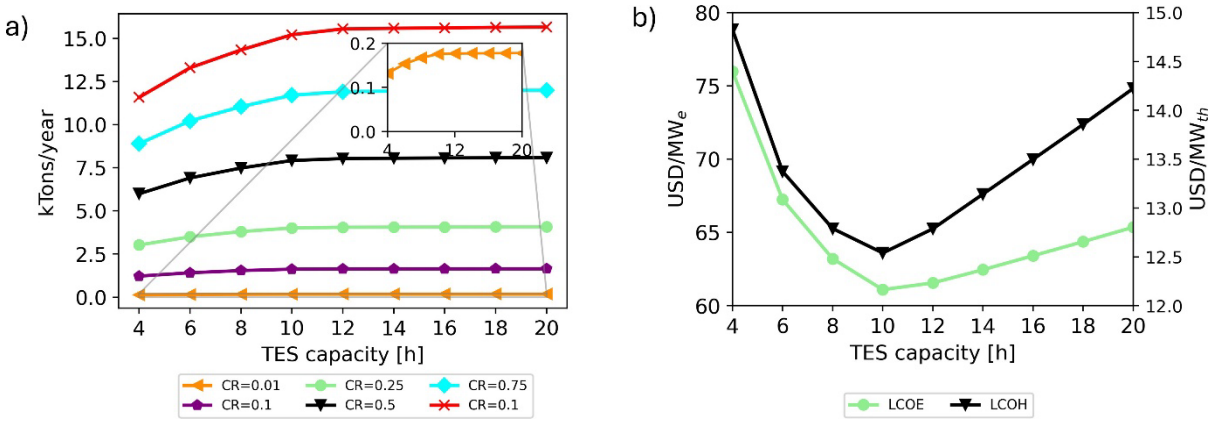

Figure 5. *(a) Annual hydrogen production concerning the TES capacity and CR and (b) techno-economic performance indicatior (LCOE and LCOH) of Gen3 CSP plant concerning the TES capacity*

Considering these aspects, with around 10 hours of TES and CR values between 0.01 and 0.2, gH_2 production ranges from 175.4 to 4053.2 kTons/year. Meanwhile, the fossil fuel energy demand of copper mining in the Atacama region is approximately 10,000 TJ/year. Therefore, with this level of gH_2 production, it would be possible to replace approximately 249.07% to 5755.58% of the fossil fuel energy demanded in the Atacama region, indicating a significant surplus of energy available from gH_2 that can be used and marketed to neighboring

industries. Additionally, only a central gH_2 plant of up to 25 MW_{dc} is needed to meet multiple times the fossil fuel energy demands of large-scale copper mining in this region.

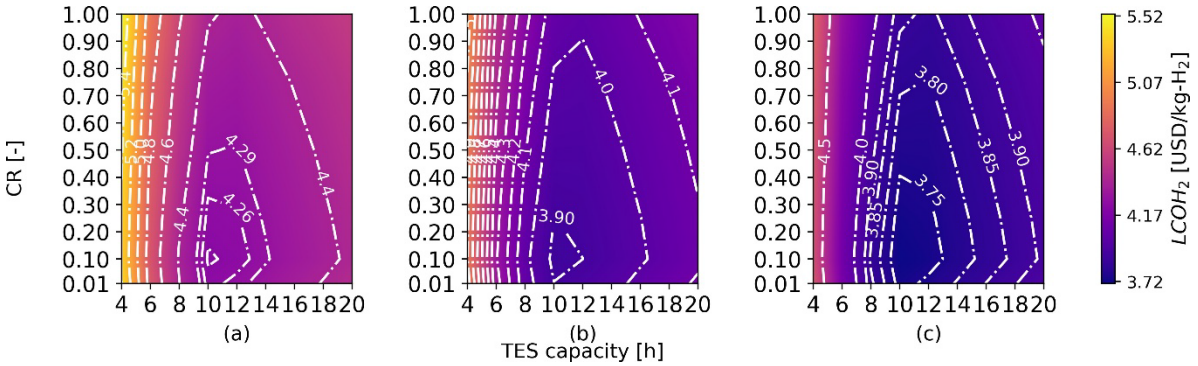

Figure 6. *$LCOH_2$ variation concerning the TES capacity, CR, and cost of each SOEC stack: (a) 300 USD/kW_{dc}, (b) 100 USD/kW_{dc}, and (c) 50 USD/kW_{dc}*

4. Conclusions

This study highlights the potential of integrating Gen3 CSP systems with SOEC for efficient hydrogen production in the Atacama Desert. Optimal performance was observed with 10 hours of TES, where further increases in storage capacity resulted in diminishing returns. The analysis indicates that maintaining a capacity ratio between 0.01 and 0.2 ensures stable hydrogen production while minimizing the $LCOH_2$. The Atacama region, with its abundant solar resources and significant industrial energy demands, particularly from copper mining, provides a strategic opportunity for deploying CSP+SOEC systems. This integration could exceed regional fossil fuel energy requirements and enable the commercialization of surplus hydrogen, contributing to the decarbonization of energy-intensive industries.

Data availability statement

Satellite data used in this work was obtained from the Solcast a DNV company.

Author contributions

Ignacio Arias: Conceptualization, Methodology, Programming, Formal Analysis, In- vestigation, Resources, Writing–Original Draft, Visualization, Funding Acquisition. Ar- mando Castillejo-Cuberos: Conceptualization, Methodology, Formal Analysis, Inves- tigation, Resources, Writing–Original Draft. J. Romero-Ramos: Conceptualization, Methodology, Formal Analysis, Investigation, Resources, Writing–Original Draft. Loreto Valenzuela: Conceptualization, Methodology, Writing–Original Draft. L.F González-Portillo: Conceptualization, Methodology, Writing–Original Draft. Jose´ Miguel Cardemil: Conceptualization, Methodology, Resources, Writing–Original Draft, Funding Acquisition. Rodrigo Escobar: Conceptualization, Methodology, Resources, Writing– Original Draft, Funding Acquisition.

Competing interests

The authors declare that they have no competing interests.

Acknowledgements

I. Arias acknowledges funding from ANID PFCHA Doctorado Nacional 2021-21210053. F. G. Battisti acknowledges the funding from ANID/CONICYT through FONDECYT Postdoctorado 2022 #3220792. A Castillejo-Cuberos acknowledges the funding from ANID through project FONDECYT Postdoctorado 2022 #3220686. The authors gratefully acknowledge the financial support from Projects ANID/FONDECYT 1231186 and 1240739 and Project ANID/FONDAP 1523A0006.

References

[1] R. 21, "Renewables 2023 global status report," Tech. Rep., 2023. [Online]. Available: https://www.ren21.net/wpcontent/uploads/2019/05/GSR2023_GlobalOverview_Full_Report_with_endnotes_web.pdf.

[2] I. Arias, A. Castillejo-Cuberos, F. G. Battisti, *et al.*, "An in-depth system-level assessment of green hydrogen production by coupling solid oxide electrolysis and solar thermal systems," *Energy Conversion and Management*, vol. 327, p. 119 537, 2025, ISSN: 0196- 8904. DOI: https://doi.org/10.1016/j.enconman.2025.119537. [Online]. Available: https://www.sciencedirect.com/science/article/pii/S0196890425000603.

[3] L. F. González-Portillo, K. Albrecht, and C. K. Ho, "Techno-economic optimization of csp plants with free-falling particle receivers," *Entropy*, vol. 23, no. 1, 2021, ISSN: 1099-4300. DOI: 10.3390/e23010076. [Online]. Available: Available: https://www.mdpi.com/1099-4300/23/1/76.

[4] P. G. Gan, W. Ye, and P. John, "System Modelling and Optimization of a Particle-Based CSP System," *The Australian National University: Canberra, Australia*, 2021.

[5] J. Chen, K. Cheng, X. Li, X. Huai, and H. Dong, "Thermodynamic evaluation and optimization of supercritical co2 brayton cycle considering recuperator types and designs," *Journal of Cleaner Production*, vol. 414, p. 137 615, 2023, ISSN: 0959-6526. DOI: https:// doi. org/ 10 . 1016 / j. jclepro. 2023 . 137615. [Online]. Available: https://www . sciencedirect.com/science/article/pii/S0959652623017730.

[6] M. J. Blanco, K. Milidonis, and A. M. Bonanos, "Updating the psa sun position algorithm," *Solar Energy*, vol. 212, pp. 339–341, 2020, ISSN: 0038-092X. DOI: https://doi.org/10.1016/j.solener.2020.10.084. [Online]. Available: https://www.sciencedirect.com/science/article/pii/S0038092X20311488.

[7] L. F. González-Portillo, V. Soria-Alcaide, K. Albrecht, C. K. Ho, and B. Mills, "Benchmark and analysis of a particle receiver 1D model," *Solar Energy*, vol. 255, pp. 301–313, May 2023, ISSN: 0038-092X. DOI: 10.1016/J.SOLENER.2023.03.046.

[8] M. Ni, M. K. Leung, and D. Y. Leung, "Parametric study of solid oxide steam electrolyzer for hydrogen production," *International Journal of Hydrogen Energy*, vol. 32, no. 13, pp. 2305–2313, 2007, ICHS-2005, ISSN: 0360-3199. DOI: https://doi.org/10.1016/j.ijhydene. 2007 . 03 . 001. [Online]. Available:https://www.sciencedirect.com/science/article/pii/S0360319907001358.

[9] H. Zhang, J. Ye, X. Hu, H. Huang, H. Wang, and J. Han, "Diffusion-reaction model and electrolysis dynamic characteristics of electrode surface and channel in solid oxide elec- trolytic cell," in *2022 9th International Forum on Electrical Engineering and Automation (IFEEA)*, 2022, pp. 813–820. DOI: 10.1109/IFEEA57288.2022.10038101.

[10] I. Arias, F. G. Battisti, J. Romero-Ramos, *et al.*, "Assessing system-level synergies be- tween photovoltaic and proton exchange membrane electrolyzers for solar-powered hy- drogen production," *Applied Energy*, vol. 368, p. 123 495, 2024, ISSN: 0306-2619. DOI: https:// doi. org/ 10 . 1016 / j. apenergy. 2024 . 123495. [Online]. Available: https://www.sciencedirect.com/science/article/pii/S030626192400878X.

[11] C. K. Ho, J. Sment, K. Albrecht, *et al.*, "Gen 3 particle pilot plant (g3p3) – high-temperature particle system for concentrating solar power (phases 1 and 2)," Nov. 2021. DOI: 10.2172/1832285. [Online]. Available: https://www.osti.gov/biblio/1832285.

[12] R. Anghilante, D. Colomar, A. Brisse, and M. Marrony, "Bottom-up cost evaluation of soec systems in the range of 10–100 mw," *International Journal of Hydrogen Energy*, vol. 43, no. 45, pp. 20 309–20 322, 2018, ISSN: 0360-3199. DOI: https://doi.org/10.1016/j.ijhydene.2018.08.161.[Online]. Available:https://www.sciencedirect.com/science/article/pii/S0360319918327368.

[13] J. H. Prosser, B. D. James, B. M. Murphy, *et al.*, "Cost analysis of hydrogen production by high-temperature solid oxide electrolysis," *International Journal of Hydrogen Energy*, vol. 49, pp. 207–227, 2024, ISSN: 0360-3199. DOI: https://doi.org/10.1016/j.ijhydene.2023.07.084. [Online]. Available: https://www.sciencedirect.com / science/article/pii/S0360319923034985.

[14] U. D. of Energy, *Technical targets for high temperature electrolysis*, Accessed on March 5, 2024, 2022. [Online]. Available: https : / / www . energy . gov / eere / fuelcells / technical-targets-high-temperature-electrolysis.

[15] M. Mohebali Nejadian, P. Ahmadi, and E. Houshfar, "Comparative optimization study of three novel integrated hydrogen production systems with SOEC, PEM, and alkaline electrolyzer," *Fuel*, vol. 336, no. November 2022, p. 126 835, 2023, ISSN: 00162361.DOI:10.1016/j.fuel.2022.126835.[Online].Available: https://doi.org/10.1016/j.fuel. 2022.126835.

[16] A. T. Mayyas, M. F. Ruth, B. S. Pivovar, G. Bender, and K. B. Wipke, "Manufacturing cost analysis for proton exchange membrane water electrolyzers," National Renewable Energy Laboratory (NREL), Tech. Rep., Aug. 2019. DOI: 10.2172/1557965. [Online]. Available: https://www.osti.gov/biblio/1557965.